Prediction of NOx in Premixed High-Pressure Lean Methane Flames with a MMC-Partially Stirred Reactor

B. Sundaram[a], A.Y.Klimenko[a], M.J.Cleary[b], U. Maas[c]

[a] *The University of Queensland, School of Mechanical and Mining Engineering, QLD 4072, Australia*
[b] *The University of Sydney, School of Aerospace, Mechanical and Mechatronic Engineering, NSW 2006, Australia*
[c] *Karlsruhe Institute of Technology, Institute of Technical Thermodynamics, BW 76131, Germany*

Volume 35, Issue 2, 2015, p.1517
Available online 23 August 2014

Proceedings of the Combustion Institute

Abstract

The multiple mapping conditioning (MMC) method is used to extend the stochastic PDF approach to the flamelet regimes of premixed combustion. MMC permits for a desired degree of flamelet-like conditions while reflecting the fluctuating nature of turbulent flames and preserving the integrity and universality of the chosen mixing model. The model is implemented in the context of the partially stirred reactor (PaSR), which is therefore generalised to have a wider range of applicability. A stochastic formulation of original MMC is deployed, where mixing of particle scalar values is conditioned on a Markovian reference variable which emulates an implied particle position relative to a flame. The model interactions with the reference variable are controlled through the flamelet localness parameter, Λ, which is also related to the ratio of diffusive to convective time scales. The model is implemented in a Monte Carlo numerical scheme using detailed GRI3.0 chemical kinetics without adjustments of kinetic coefficients. Predictions of NOx emissions are validated against experimental data for a lean premixed high-pressure combustor in which reactions fall between the flamelet and distributed regimes. There is good agreement between model predictions and experimental data.

Keywords: Multiple Mapping Conditioning, Probability Density Function, Flamelet, Turbulent Premixed Combustion, Combined Reactors

1. Introduction

The great attraction of probability density function (PDF) models [1] is that, unlike many other turbulent combustion models, species chemical source terms appear in closed form and do not require additional modelling. It can therefore be argued that PDF models are generally not constrained to specific turbulent combustion regimes. However, the PDF model equations introduce an unclosed conditional scalar dissipation term, and in the context of a Monte Carlo numerical scheme that term is modelled via a mixing operation. The predictive ability of PDF methods for the non-premixed combustion regime is well established [2].

Email address: brruntha.sundaram@uqconnect.edu.au (B. Sundaram[a])

Conversely, their applicability for premixed flames with high Damköhler numbers has been questioned [3] on the basis of the existence of flamelet regimes. Laminar flamelet models (LFM) [4, 5] assume that the turbulent flame is comprised of locally one-dimensional laminar flamelets. LFMs are economical for engineering applications as the laminar flames can be precomputed for subsequent use in turbulent flow simulations [6]. While the LFM represents a rigorous limit for cases when the Karlovitz number approaches zero, realistic premixed flames can possess flamelet features and simultaneously involve strain, stretch, curvature and possible local extinctions. Modelling of these phenomena may be suited to PDF methods which are generally better at handling more distributed flames. There is a large volume of literature dedicated to asymptotic studies of flamelets disturbed by non-uniform fluid flows [4, 7, 8, 9, 10]. Due to the nature of asymptotic analysis, these works are necessarily limited to studies on small perturbations of laminar flamelets.

In light of the issues mentioned above, several methods have been suggested for accommodating the flamelet regime within the context of PDF models. For example, Pope and Anand [11] and Haworth [12] model the joint velocity-progress variable PDF with embedded premixed structures to account for the tight reactive-diffusive coupling in the flame front and a conventional mixing model for the distributed reaction regime. Such approaches result in a model for both the flamelets and distributed reaction regimes. Klimenko and Pope [13] replace conventional (and conservative) mixing with competitive mixing to emulate the invasion conditions in turbulent premixed flames in the flamelet regime and demonstrate how the propagation speed can be made consistent with existing experimental data [14]. Zoller *et al.* [15] propose a model for the corrugated flamelet regime which combines the BML approach and a flame surface density closure, with a premixed LFM applied when the reaction progress variable reaches unity.

It is the aim of the present work to incorporate flamelet features into the PDF methodology with the aid of the multiple mapping conditioning (MMC) model [16, 17]. MMC is a PDF model which uses independent reference variables with links to physical parameters of the flow to enforce localness in the mixing model. In the context of premixed flames the enforcement of localness is used to avoid mixing between burned and unburned particles across the flame front. Pope [18] introduces the shadow position mixing model (SPMM), which makes use of alternative, *shadow* trajectories of notional particles. SPMM is an MMC-type model which allows the free selection of a localisation parameter and is expected to be efficient in emulating joint scalar-velocity statistics. In the current paper we introduce an MMC model which follows the original stochastic formulation [16]. In the suggested model the reference variable represents an *implied* particle position with respect to the flame front, which has some conceptual resemblance to the use of reference variables in SPMM. Using *implied* position only permits the simulation of flamelet-like conditions and does not account for spatial transport.

The breadth of model validation data for premixed turbulent flames is relatively limited when compared to the availability of data for non-premixed turbulent flames. This shortage is gradually being addressed through high quality experiments such as those for the Sydney piloted premixed jet burner(PPJB) [19] and

the Cambridge stratified swirl burner [20], as well as experimental [14] and DNS [21] premixed databases. A number of RANS-PDF and LES-PDF modellers (e.g. Refs[22, 23, 24, 25, 26, 27]) have made contributions by validating against these and other experimental databases but once again the body of modelling research is relatively limited when compared to that for non-premixed combustion.

Combustion in a partially stirred reactor (PaSR) is an alternative platform for validation of PDF models. The turbulence is assumed to be statistically homogeneous and isotropic, so that turbulence-chemistry interactions can be investigated without the need for CFD. The PaSR tends to a plug flow reactor (PFR) in the limit of slow mixing and to a perfectly stirred reactor (PSR) in the limit of very fast mixing. An early example of a stirred tank reactor which incorporates mixing, flow-through and reaction is found in Levenspiel and Spielman [28]. The work of Correa [29, 30] on premixed methane combustion and Chen [31] on non-premixed hydrogen combustion establishes the PaSR as a tool for analysis of turbulence-chemistry interactions and as a test bed for PDF models. For example, a PaSR is used by Bender *et al.* [32] to study the coupling of chemistry and turbulent mixing for both detailed and reduced chemical kinetics, and a projection scheme is introduced for mixing models to be used with the intrinsic low dimensional manifold (ILDM) method [33]. As well as being a basis for model development, the PaSR is an important model in itself with application to gas turbine combustors and other chemical reactors. Cannon *et al.* [34] use a PDF-PaSR model to predict carbon monoxide (CO) and nitric oxide (NOx) emissions for a range of lean and stoichiometric premixed conditions with several reduced kinetics mechanisms in conjunction with in-situ adapative tabulation (ISAT) [35] while Bhave *et al.* [36] use a conceptually similar stochastic reaction model to predict CO emissions for a HCCI engine.

In the remainder of this paper we develop a new MMC-PaSR model which is implemented in a Monte Carlo numerical scheme and then validated against experimental data for NOx emissions from a lean high-pressure methane combustor. The model is demonstrated for a range of combustor equivalence ratios and inlet temperatures.

The paper is organized as follows. The next section presents an overview of MMC along with the incorporation of the reference variable representing position which extends MMC to the flamelet regimes of premixed combustion. Section 3 describes the experimental conditions for model validation and is followed by Section 4 on the numerical implementation of the MMC-PaSR. Results and discussion on NOx emissions and an analysis of the model parameters are contained in Section 5. Conclusions follow in Section 6.

2. Theoretical Description of MMC-PaSR

Multiple mapping conditioning was first introduced [16] as a unification of the PDF, conditional moment closure (CMC) [37] and mapping closure [38, 39]. The basic MMC framework has since been expanded to encompass a number of specific models (e.g. Refs[18, 40, 41, 42, 43, 44, 45]). Both deterministic and stochastic MMC formulations are presented as subsets of original MMC in [16]. Deterministic MMC is the

natural extension of CMC while stochastic MMC is a complete joint PDF method with MMC playing the role of a mixing model enforcing localness and possibly other desired properties on mixing. The feature common to all MMC models is the use of reference variables which are related to the physical quantities in turbulent combustion. Two forms of MMC are distinguished; original and generalised [46]. While, in original MMC conditioning is necessarily performed on all reference variables evolving according with a Markov vector process, in generalised MMC, conditioning of the mixing operator is performed on a subset of reference variables. This means that reference variables in generalised versions of the model can in principle be represented by any useful physical quantities.

The present work introduces a model which follows the methodology of the original stochastic version of MMC [16]. The model is given by:

$$d\xi^* = udt + bd\omega^* \tag{1}$$

where $b = \lambda u$

$$dY_I^* = (W_I^* + S_I^*)dt \tag{2}$$

$$\langle S_I^* |\ \xi^* = \xi \rangle = 0 \tag{3}$$

The MMC reference variable is denoted as ξ, mass fraction of species is Y and time is t. In the equations above, "*" indicates that a quantity is stochastic, u is effective drift velocity which can be estimated as a characteristic length L divided by residence time, b is effective diffusion and ω_I^* is a Wiener processes in the reference space. The term λ is an additional parameter specific to this formulation of the MMC-PaSR. The influence of λ is discussed in detail further on in Section 2. Equation (1) models the evolution of the reference variable, which has the dimension of length. Equation (2) governs transport in scalar space due to chemical reaction W_I and a mixing operation S_I. Any set of reactions from a single step to full chemistry can be implemented on the set of particles as part of W_I. Mixing is also not restricted to any specific model and models such as Curl's [47] and Interaction by Exchange with the Mean (IEM) [48] can be used. The MMC version of such conventional models is described by Eq. (3) defining the localness condition in the reference space, which is the crux of MMC.

The first and second terms on the right hand side of Eq. (1) are drift and diffusion, respectively. In the current model, the reference variable serves as a proxy for a relative particle position in the vicinity of the premixed reaction zone. Particle positions in the reference space ξ are traced, and only the particles closest in ξ-space are permitted to mix. MMC prevents mixing between particles which occupy mutually remote locations in a combusting system. The mixing scheme is consistently applied to all scalars. This conditioning ensures desirable properties such as localness, independence of the reference (ξ^*) and the composition variables (Y_I^*), and linearity. This use of the reference variable has conceptual similarity with SPMM [18] although our implementation is different as we do not attempt investigation of spatial transport

properties. As the reference variable does not directly simulate physical position, spatial transport is not modelled and the current formulation does not contain a linear relaxation term in Eq. (1).

It is clear that the model specified by Eq. (1)-(3) falls into the category of original MMC: there is a single Markov reference variable on which conditioning is performed. As MMC theory [16] indicates, the conditional expectation $Q_I = \langle Y_I^* | \xi \rangle$ satisfies the deterministic version of the MMC model:

$$\frac{\partial Q_I}{\partial t} + u\frac{\partial Q_I}{\partial \xi} - B\frac{\partial^2 Q_I}{\partial \xi^2} = W_I \tag{4}$$

where $B = b^2/2$ is the diffusion coefficient in the reference space. Since we consider stochastic MMC here, Y_I^* deviates from Q_I, but mixing operators with a very small characteristic time τ_S can enforce proximity of Y_I^* to Q_I. If required, the stochastic version of MMC can approach the deterministic version as τ_S approaces zero. Equation (4) is essentially CMC with progress-variable type conditioning [37] which in this case is equivalent to the flamelet model (assuming consistent selection of the model coefficients). The parameter λ which is first introduced alongside Eq. (1) is responsible for emulating the degree of turbulent stirring of fluid parcels. In the present formulation, the coupled effect of changing b and u occurs only through λ. Larger λ would permit a greater entrainment of the unburned mixture into the average position of the flame. As mixing is always localised in ξ-space, small values of λ enforce more localised mixing which is more strict in preventing the direct mixture of unburned and burned mixtures, implying a higher level of compositional localness. For even smaller values of λ less than a certain critical value λ_c, the diffusion is dominated by the drift and the flame is blown off. The case of $\lambda = \lambda_c$ therefore corresponds to maximal enforcement of compositional localness or flamelet-like conditions such that a reaction zone can be sustained. The normalised parameter $\Lambda = \lambda_c/\lambda$ indicates a degree of "flamelet-ness" enforced on the PDF model. It must be noted that flamelet-ness is not equated to blow-off. As Λ approaches unity, the model bears increasing resemblance to laminar flamelets. If Λ is reduced, stirring is increased and we depart from the flamelet regime. Thus we nominate the term flamelet localness to describe Λ.

All MMC models considered previously have a parameter characterising localness (or non-localness) [18, 45, 46, 49]. The definition of localness differs depending on the application and specifics of the model. Here, the flamelet localness Λ has conceptual similarity with previous MMC works but is specifically defined for this model. In an early stochastic version of MMC [49], localness is linked to the ratio between minor and major dissipation timescales. This timescale ratio bears similarity to another ratio present in the MMC-PaSR model τ_S/τ_{res} (where τ_{res} is residence time). In the context of modelling turbulent premixed combustion, it appears that the degree of flamelet localness effected through Λ is of more importance while τ_S/τ_{res} has a secondary effect.

If Λ is suffiently small, the MMC-PaSR effectively becomes a PaSR. In this case, a low ratio of τ_S/τ_{res} enforces conditions which correspond to a PSR. If $\Lambda \approx 1$, flamelet-like conditions are maximally enforced while a low ratio of τ_S/τ_c (where τ_c is a characteristic chemical time) negates fluctuations around flamelet-like

solutions and enforces proximity of Y_I^* to Q_I.

Figure 1 illustrates the effect of Λ for a temperature-based progress variable plotted against the reference variable. The conditions shown are for τ_{res} of 0.01 s, inlet temperature of 617 K, pressure of 10.4 atm and equivalence ratio of 0.5 based on a high pressure lean premixed experimental case which is discussed further on in Section 3. It demonstrates the departure of the model from the flamelet-type condition towards a PaSR in the reaction zone followed by a plug flow zone where mixing becomes position dependent. Specifically, it can be seen that for $\Lambda \approx 1$, there is a high degree of localisation and mixing between burned and unburned quantities can only occur in a sequence of multiple mixing events through the reaction band. Localised mixing allows the growth of the plug flow zone beyond this flamelet region. As relative stirring or Λ is decreased, the reaction zone becomes less flamelet like and the stirred zone dominates while the plug flow zone is delayed. Therefore, the MMC-PaSR can produce results which span the PSR, PaSR and PFR limits and at the same time can reproduce flamelet-like conditions.

3. Implementation of MMC-PaSR

The MMC-PaSR model is implemented using a Monte-Carlo particle method. The PDF is represented by n_p Pope particles which are initialised at specified conditions for a given thermochemistry with any desired distribution in reference space. In principle, it is possible to tune mixing based on one or more reference variables and control the quantity and location of single or multiple injection points. Essentially the same model (MMC-PaSR) can handle premixed, partially premixed or non-premixed injections. The particle replacement scheme can be modified to suit a desired distribution or for weighted removal from various zones.

For each time step Δt, the increments of the particle properties are decomposed into flowthrough, mixing and reaction. These substeps occur successively and the conditions at the preceding substep set the conditions for the current substep. In this work, particle scalars are initialised at equilibrium and have a random uniform distribution of $\xi \subset [0, L]$, where the characteristic length $L = u\tau_{res}$.

At each time step, particle reference position is incremented according to Eq. (1). Flowthrough, or the number of particles replaced at each timestep, is controlled through τ_{res} such that the average number of particles replaced is $\Delta n = n_p \Delta t/\tau_{res}$. In the current implementation, particles with the largest values in reference space are removed. Upon removal, the reference variable and scalars are reset to zero and unburned conditions respectively, simulating a single injection point at $\xi = 0$, in line with the configuration of the selected combustor. As in this case, recirculation prior to the injection point is not deemed to physically exist in the combustor, a reflective wall is applied at the injection point to prevent the formation of an appendix produced by diffusion of particles into negative reference space due the random walk term in Eq. (1).

Particles mix based on a conditioned Modified Curl mixing model [50]. In this MMC-Curl model, the mixing extent α is assigned to a random value between zero and one. Particles are ordered in ξ-space, paired

and mixed according to

$$\begin{cases} Y^p(t+\Delta t) = (1-\alpha)Y^p + \frac{1}{2}\alpha(Y^p + Y^q) \\ Y^q(t+\Delta t) = (1-\alpha)Y^q + \frac{1}{2}\alpha(Y^p + Y^q) \end{cases} \tag{5}$$

assuming that particles p and q are a mixing couple.

The characteristic time of the mixing operator which can also be called minor dissipation time or micro-mixing time is specified through selection of α by

$$\tau_S = \frac{4\Delta t}{2\langle\alpha\rangle - \langle\alpha\rangle^2} \tag{6}$$

To avoid common situations where adjustments in kinetics coefficients compensate for and hide modelling deficiencies, we use a comprehensive standard mechanism. Chemical source terms are evaluated from the GRI3.0 kinetics scheme [51] containing 53 species and 325 reaction steps including NOx and time integration is performed by the stiff ODE solver CVODE [52]. All species and reaction steps are simulated in this work.

4. Results and Discussion

MMC-PaSR simulations are performed for methane flames at i) a pressure of 10.4 atm and for inlet temperatures of 617 K, 533 K and 311 K and ii) a temperature of 322 K and for pressures of 10.3 atm and 6 atm. Convergent and stable simulations are achieved using 512 fully reacting particles for twice the duration of the residence time which varies depending on the case. The influence of lambda is stronger than mixing time, provided it is selected from a physically correct range. Here, mixing time is selected to be greater than the reaction time but less than residence time and is fixed as $1{\times}10^{-5}$ s by mixing 90% of particles to an average extent of 0.2. Following the reporting procedure for conventional gas turbine combustors, which is also used in [53], the NOx values shown in all figures have been corrected to a dry 15% reference oxygen level unless otherwise specified.

For the accurate and transparent presentation of results, we describe and discuss the outcomes in terms of both λ and the flamelet localness Λ, which is λ_c/λ, since there is a greater uncertainty in determining the exact value of λ_c. As it is difficult to predict the exact value of λ_c in simulations due to the inherent stochasticity of the MMC-PaSR, we present an estimate of Λ where relevant. While Λ has a conceptual significance and determines the degree of flameletness, λ indicates the balance of drift between turbulent stirring and is expected to be more influenced by fluid mechanics rather than by the chemistry of the situation. In this section, the influence of λ on NOx formation and deviation of the MMC-PaSR from flamelet-like conditions into PaSR and PFR-type situations is first explored. Following on from this, the ability of the MMC-PaSR to match the average NOx recorded at the combustor exit is demonstrated. To distinguish whether improvements in results are due to kinetics or the new MMC-PaSR model, we implement a PSR-PFR similar to that of Leonard and Correa [53] with GRI3.0 chemistry. The PSR-PFR results with

GRI3.0 is very similar to the simulation results reported by Leonard and Correa [53], demonstrating that the use of detailed chemistry by itself does not necessarily lead to better predictions.

Figure 2 shows the predicted MMC-PaSR results alongside experimental data of NOx for the 10.4 atm, 617 K case, and illustrates the impact of modifying λ. All predictions shown here are for fully combusting, statistically stationary cases and species concentrations are sampled at the combustor exit (where $\xi > 0.85$L). The MMC-PaSR curves converge towards the critical, flamelet-like limit (where Λ=1) as the value of λ is decreased to a value ranging between 0.015 to 0.02 $s^{-1/2}$ for this case. The curves for λ_c are close to that of $\lambda = 0.025$ $s^{-1/2}$ and are not included in Fig. 2 for visual clarity. A further reduction below λ of 0.015 $s^{-1/2}$ results in flame blowoff for all equivalence ratios. Similar trends of convergence for NOx predictions with increasing localisation are observed for the lower inlet temperatures. The presence of several experimental points beyond $\lambda = 0.05$ show that an increase of λ permits stable combustion but excessive stirring alters NOx production. The value of λ in this case must be kept relatively close to λ_c to preserve flameletness. For a large λ mixing between unburned and burned scalars is more likely and we observe a more distributed reaction zone and a decrease in NOx. Therefore, large λ causes the model to move away from the flamelet limit towards a PaSR.

In Fig. 3, the development of NOx through the length of the combustor (i.e. along the reference variable) is shown for five values of λ ranging between 0.025 and 0.125 $s^{-1/2}$ or Λ ranging between 0.6 and 0.12. This corresponds to the case with an equivalence ratio of 0.7 shown in Fig. 2. Under these conditions, the critical lambda λ_c is approximately 0.015. In this series of figures (Fig. 3), a stirred zone and a plug flow zone are distinguished. For $\lambda = 0.025$ $s^{-1/2}$ which is the closest stable point still greater than λ_c, a very small stirred region is observed from $\xi = 0$. As λ increases, this stirred zone broadens. It appears that a larger λ permits more entrainment of the unburned mixture into the average position of the flame, allowing higher fluctuations and resulting in an increasingly PaSR-like situation near the inlet. The increased stirring effected through a higher *lambda* produces a higher average NOx in the stirred zone. The development of NOx in the initial well stirred zone is followed by an almost linear increase in the pollutant which approximates its evolution according to a PFR. In addition to initialising NOx concentrations at the interface between the PaSR and PFR zones, λ affects the position of the interface and the rate of NOx accumulation in the PFR. It is clear that both PaSR and PFR zones contribute to the formation of NOx throughout the domain influencing emissions at the exit.

Figure 4 shows NOx as a function of equivalence ratio and the inlet temperatures of 617 K, 533 K and 311 K at a pressure of 10.4 atm. Although residence times for all three cases are approximated to be 10 ms based on the flow rates provided in [53], there was a 13% difference between the highest and lowest flow rates (corresponding to 617 K and 311 K respectively). Sensitivity tests show that $\pm$10% variation of τ_{res} in the MMC-PaSR allows most of the experimental data points to fall within the limits of uncertainty caused by varying flow rates. The residence time estimate of 10 ms is therefore valid. For all three inlet temperatures MMC-PaSR simulations with a $\lambda = 0.05$ $s^{-1/2}$ with a corresponding Λ of approximately 0.3

yield the best match when compared with experimental NOx emissions, and show improvement compared to the previous PSR-PFR network [53]. This consistency in results supports the notion that λ is a fluid dynamics parameter which controls the balance between diffusion and drift.

Similarly to Fig. 4, Fig. 5 shows NOx predictions for pressures of 10.3 atm and 6 atm at an inlet temperature of 322 K. The residence times for the 10.3 atm and 6 atm cases are calculated to be approximately 10 ms and 15 ms respectively based on the flow rates. For the 10.3 atm case, the optimal λ was 0.125 $s^{-1/2}$ with a Λ of approximately 0.2. The λ and Λ for the 6 atm case were approximately 0.4 $s^{-1/2}$ and 0.0625. For both cases here and in the previous cases with varying temperature, λ_c was in the range of 0.015 to 0.025 $s^{-1/2}$.

We find that MMC localisation in a position-like reference space is essential for the correct reproduction of the trends of this particular experiment. While a corresponding time-like reference variable could have been used by dividing the current position-like reference variable by a constant, this would not have functionally affected the results. It is expected that principles drawn from this formulation of the MMC-PaSR will allow the prediction of trends in pollutant emissions - NOx, CO and CO_2 - from gas combustors with one or more injection points using full chemical kinetics and simplified fluid mechanics. We also expect that future pdf simulations for inhomogeneous premixed flows will benefit from the possibility of enforcing flamelet-like conditions by conditioning mixing on a similar position-like reference variable, although this is beyond the scope of the current work.

5. Conclusions

In this work, we apply a stochastic PDF approach to simulate premixed flames in the context of a PaSR, and exploit the ability of the MMC model to localise mixing and enforce flamelet-like conditions on conditional expectations as necessary. The principle step of this approach is the incorporation of flamelet conditions into the PDF framework without violating the principles of linearity and independence of the mixing model.

The MMC-PaSR differs from the conventional PaSR through the introduction of a reference variable ξ which is influenced by the flamelet localness parameter Λ. The reference variable emulates physical position of a Lagrangian particle with respect to the flame. The selection of Λ that is close to unity (i.e. $\lambda \approx \lambda_c$ and $\lambda \geq \lambda_c$) allows the MMC-PaSR to mimic flamelet-like conditions but compared to the LFM, the MMC-PaSR permits the necessary degree of fluctuations in scalars. Various values of λ are tested for a lean high-pressure methane-air flame for three inlet temperatures and two pressures. NOx is well predicted for all cases using the standard GRI3.0 mechanism. Optimal results are obtained by allowing the MMC-PaSR to emulate a substantial degree flamelet-ness while permitting a noticeable level of fluctuations.

Acknowledgements

This work is supported by the Australian Research Council under grant number DP120102294.

References

[1] S. B. Pope, Prog. Energy Combust. Sci. 11 (1985) 119–192.

[2] D. C. Haworth, Prog. Energy Combust. Sci. 36 (2010) 168–259.

[3] N. Peters, Proc. Combust. Inst. 32 (2009) 1–25.

[4] V. R. Kuznetsov, V. A. Sabelnikov, Turbulence and Combustion, Hemisphere Publishing Company, New York, USA, 1990.

[5] N. Peters, Available, Cambridge University Press, Cambridge, UK, 2000.

[6] H. Pitsch, M. Chen, N. Peters, Proc. Combust. Inst. 27 (1998) 1057–1064.

[7] P. Clavin, F. A. Williams, Jrnl. Fluid Mech. 116 (1982) 251–282.

[8] M. Matalon, B. J. Matkowsky, Jrnl. Fluid Mech. 124 (1982) 239–259.

[9] G. I. Sivashinsky, Combust. Sci. Tech. 62 (1988) 77–96.

[10] A. G. Class, B. J. Matkowsky, A. Y. Klimenko, Jrnl. Fluid Mech. 4991 (2003) 11–49.

[11] S. B. Pope, M. S. Anand, Proc. Combust. Inst. 20 (1985) 403–410.

[12] D. C. Haworth, Proc. 2000 Summer Prog. DC (2000) 145–156.

[13] A. Y. Klimenko, S. B. Pope, Combust. Theory Mod. 16 (2012) 679–714.

[14] D. Bradley, A. C. K. Lau, M. Lawes, Phil. Trans. R. Soc. Lond. A 338 (1992) 359–387.

[15] B. T. Zoller, M. L. Hack, P. Jenny, Proc. Combust. Inst. 34 (2013) 1421–1428.

[16] A. Y. Klimenko, S. B. Pope, Phys. Fluids 15 (2003) 1907–1925.

[17] M. J. Cleary, A. Y. Klimenko, Turbulent Combustion Modelling Advances, New Trends and Perspectives, in T. Echekki and E. Mastorakos (eds) Springer, New York, 2011.

[18] S. B. Pope, Phys. Fluids 25 (2013) 110803.

[19] M. J. Dunn, A. R. Masri, R. W. Bilger, R. S. Barlow, G.-H. Wang, Proc. Combust. Inst. 32 (2009) 1779–1786.

[20] M. S. Sweeneu, S. Hochgreb, R. S. Barlow, Combust. Flame 158 (2011) 935–948.

[21] E. R. Hawkes, J. H. Chen, Combust. Flame 138 (2004) 242–258.

[22] S. M. Cannon, B. S. Brewster, L. D. Smoot, Combust. Flame 119 (1999) 233–252.

[23] R. P. Lindstedt, E. M. Vaos, Combust. Flame 145 (2006) 495–511.

[24] M. Stöllinger, S. Heinz, Monte Carlo Methods Appl. 14 (2008) 343–377.

[25] S. L. Yilmaz, M. B. Nik, P. Givi, P. A. Strakey, Jrnl. Prop. Power. 26 (2010) 84–93.

[26] D. H. Rowinski, S. B. Pope, Combust. Theory Mod. 17 (2013) 610–656.

[27] I. A. Dodoulas, S. Navarro-Martinez, Flow Turb. Combust. 90 (2013) 645–678.

[28] O. Levenspiel, L. A. Spielman, CHem. Eng. Sci. 20 (1965) 247–254.

[29] S. M. Correa, Combust. Flame 93 (1993) 41–60.

[30] S. M. Correa, M. E. Braaten, Combust. Flame 94 (1993) 469–486.

[31] J.-Y. Chen, Combust. Sci. Tech. 122 (1997) 63–94.

[32] R. Bender, T. Blasenbrey, U. Maas, Proc. Combust. Inst. 28 (2000) 101–106.

[33] U. Maas, S. B. Pope, Proc. Combust. Inst. 25 (1994) 1349–1356.

[34] S. M. Cannon, B. S. Brewster, L. D. Smoot, Combust. Flame 113 (1998) 135–146.

[35] S. B. Pope, Combust. Theory Mod. 1 (1997) 41–63.

[36] A. Bhave, M. Kraft, L. Montorsi, F. Mauss, Combust. Flame 144 (2006) 634–637.

[37] A. Y. Klimenko, R. W. Bilger, Prog. Energy Combust. Sci. 25 (1999) 595–687.

[38] H. Chen, S. Chen, R. H. Kraichnan, Phys. Rev. Lett. 63 (1989) 2657–2660.

[39] S. B. Pope, Theory Comp. Fluid Dyn. 2 (1991) 255–270.

[40] M. J. Cleary, A. Kronenburg, Combust. Flame 151 (2007) 623–638.

[41] M. J. Cleary, A. Y. Klimenko, J. Janicka, M. Pfitzner, Proc. Combust. Inst. 32 (2009) 1499–1507.

[42] P. Vaishnavi, A. Kronenburg, Combust. Flame 10 (2010) 1863–1865.

[43] K. Vogiatzaki, A. Kronenburg, S. Navarro-Martinez, W. P. Jones, Proc. Combust. Inst. 33 (2011) 1523–1531.

[44] A. Wandel, R. P. Lindstedt, Proc. Combust. Inst. 34 (2013) 1365–1372.

[45] Y. Ge, M. J. Cleary, A. Y. Klimenko, Proc. Combust. Inst. 34 (2013) 1325–1332.

[46] M. J. Cleary, A. Y. Klimenko, Flow Turb. Combust. 82 (2009) 477–491.

[47] R. L. Curl, Aiche Journal 9 (1963) 175–181.

[48] C. Dopazo, Phys. Fluids 18 (1975) 397–410.

[49] A. Wandel, A. Y. Klimenko, Phys. Fluids 17 (2005) 128105.

[50] J. Janicka, W. Kolbe, W. Kollman, Jrnl. Non-Equilib. Thermodyn. 4 (1977) 47–66.

[51] G. P. Smith, D. M. Golden, M. Frenklach, N. W. Moriarty, B. Eiteneer, M. Goldenberg, C. T. Bowman, R. K. Hanson, S. Song, W. C. J. Gardiner, V. V. Lissianski, Z. Qin, <http://www.me.berkeley.edu/gri_mech/>.

[52] S. Cohen, A. C. Hindmarsh, C. Computers in Physics (1996) 138–143.

[53] G. Leonard, S. Correa, Jrnl. Prop. Power 8 (1992) 69–74.

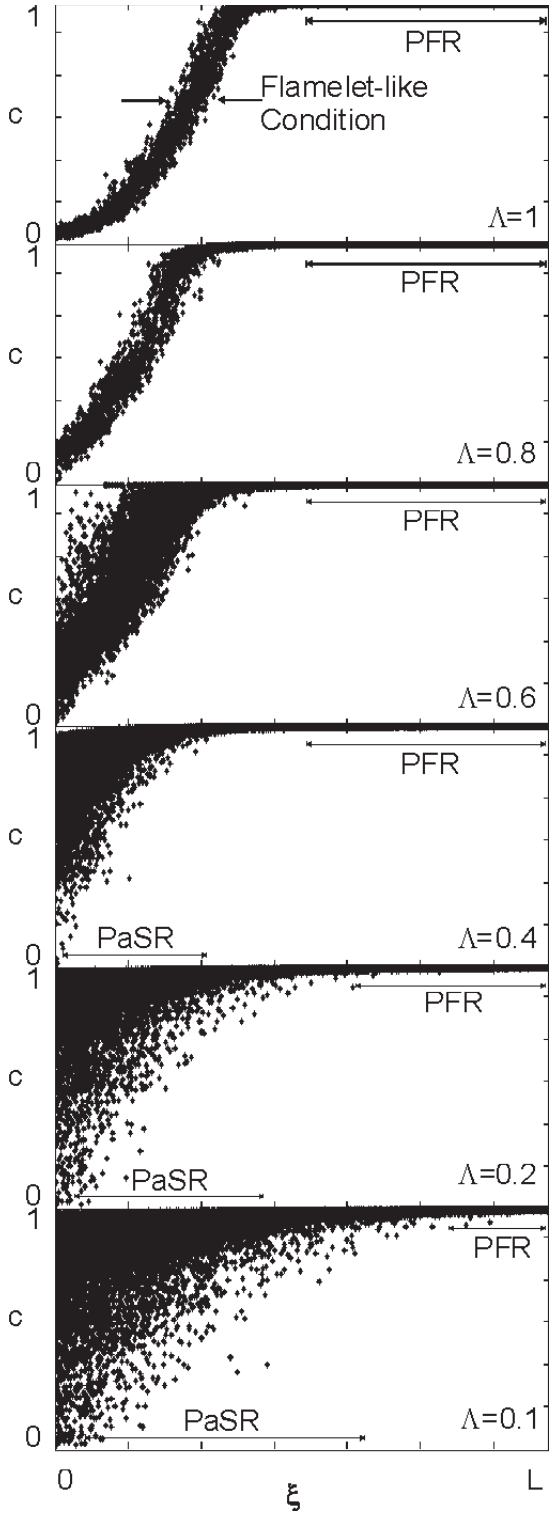

Figure 1: Temperature-based reaction progress variable (c) versus the reference variable (ξ) for decreasing Λ showing departure of MMC-PaSR from flamelet conditions to PaSR conditions. The length of the plug flow zone beyond the reaction zone is controlled by Λ and τ_{res}.

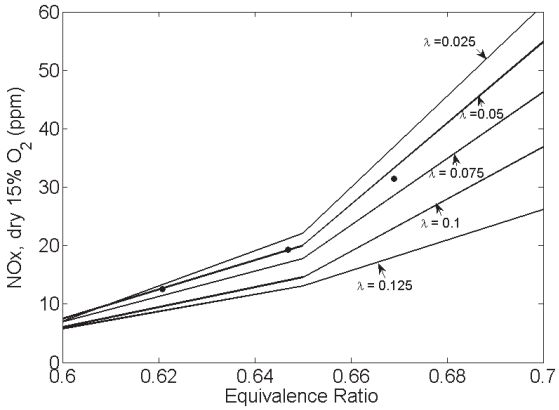

Figure 2: Dry, corrected NOx as a function of equivalence ratio for P = 10.4 atm, τ_{res} = 10 ms and T = 617 K. Experimental data (circles) and MMC-PaSR results (solid lines) are shown for λ ranging from 0.025 to 0.125.

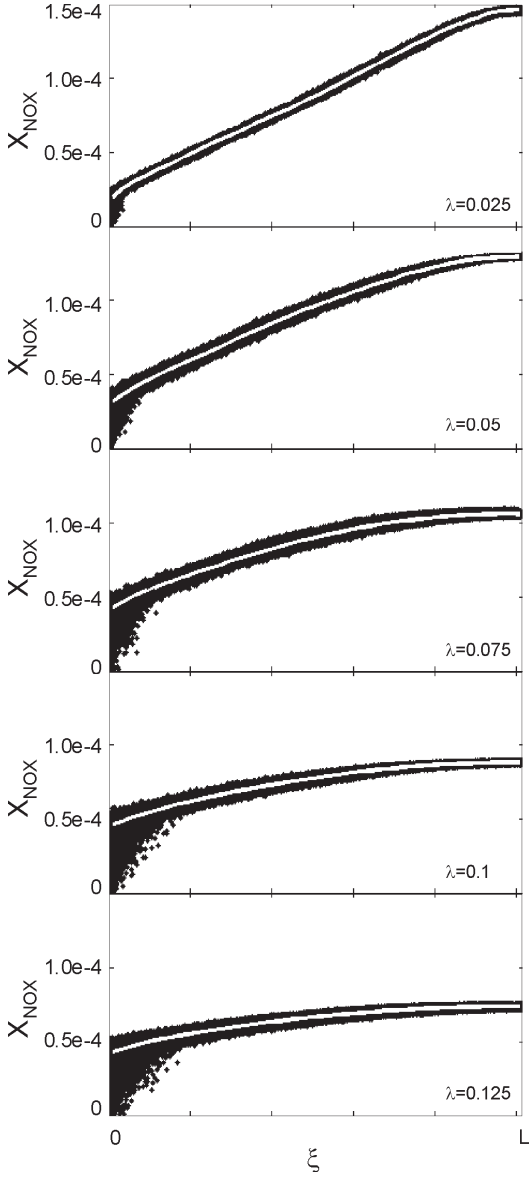

Figure 3: NOx mole fraction (X_{NOX}) versus reference variable (ξ) for increasing λ from 0.025 up to 0.125 showing departure of MMC-PaSR from flamelet-like conditions for P = 10.4 atm, τ_{res} = 10 ms, T = 617 K and equivalence ratio of 0.7. The PDF (black dots) and conditional mean (white line) are shown.

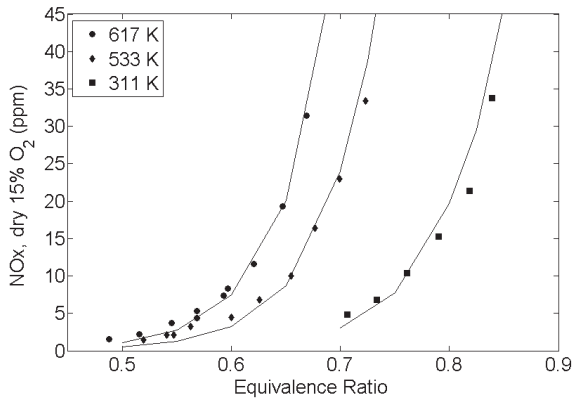

Figure 4: Dry, corrected NOx as a function of equivalence ratio for P = 10.4 atm, τ_{res} = 10 ms for inlet temperatures of 311 K (squares), 533 K (diamonds) and 617 K (circles). MMC-PaSR results (solid lines) are based on a single value of $\lambda = 0.05$ $s^{-1/2}$.

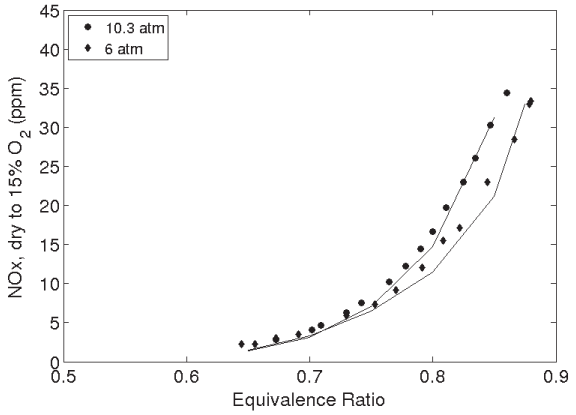

Figure 5: Dry, corrected NOx as a function of equivalence ratio for T = 322 K, for pressures of 10.3 atm (circles) and 6 atm (diamonds). MMC-PaSR results (solid lines) are based on λ of 0.125 and 0.4 $s^{-1/2}$ for the 10.3 atm and 6 atm cases respectively.